Article

Atmospheric Deposition of Mercury and Methylmercury to Landscapes and Waterbodies of the Athabasca Oil Sands Region

Jane Kirk, Derek C.G. Muir, Amber Gleason, Xiaowa Wang, Richard Frank, Igor Lehnherr, and Fred Wrona

Environ. Sci. Technol., **Just Accepted Manuscript** • DOI: 10.1021/es500986r • Publication Date (Web): 29 May 2014

Atmospheric Deposition of Mercury and Methylmercury to Landscapes and Waterbodies of the Athabasca Oil Sands Region

Jane L. Kirk[1*], Derek C. G. Muir[1], Amber Gleason[1], Xiaowa Wang[1], Richard A. Frank[1], Igor Lehnherr[2], Fred Wrona[3]

[1]*Environment Canada, Aquatic Contaminants Research Division, Burlington, ON, L7R 4A6, Canada*
[2]*Department of Earth and Environmental Sciences, University of Waterloo, Waterloo, ON, N2L 3G1, Canada*
[3]*Environment Canada, Water and Climate Impacts Research Centre, University of Victoria 3800 Finnerty Road, Victoria, BC, V8P 5C2, Canada*

*Corresponding author: JL Kirk, Environment Canada, Aquatic Contaminants Research Division, Burlington, ON, L7R 4A6, Canada Phone: 905 336 4712 E-mail: Jane.Kirk@ec.gc.ca

Abstract

Atmospheric deposition of metals originating from a variety of sources, including bitumen upgrading facilities and blowing dusts from landscape disturbances is of concern in the Athabasca oil sands region of northern Alberta, Canada. Mercury (Hg) is of particular interest as methylmercury (MeHg), a neurotoxin which bioaccumulates through foodwebs, can reach levels in fish and wildlife that may pose health risks to human consumers. We used spring-time sampling of the accumulated snowpack at sites located varying distances from the major developments to estimate winter 2012 Hg loadings to a ~20 000 km^2 area of the Athabasca oil sands region. Total Hg (THg; all forms of Hg in a sample) loads were predominantly particulate-bound (79 ± 12%) and increased with proximity to major developments, reaching up to 1000 ng m^{-2}. MeHg loads increased in a similar fashion, reaching up to 19 ng m^{-2} and suggesting that oil sands developments are a direct source of MeHg to local landscapes and water bodies. Deposition maps, created by interpolation of measured Hg loads using geostatistical software, demonstrated that deposition resembled a bullseye pattern on the landscape, with areas of maximum THg and MeHg located primarily between the Muskeg and Steepbank rivers. Snowpack concentrations of THg and MeHg were significantly correlated ($r = 0.45$-0.88, $p<0.01$) with numerous parameters, including total suspended solids (TSS), metals known to be emitted in high quantities from the upgraders (vanadium, nickel, and zinc) and crustal elements (aluminum, iron, and lanthanum), which were also elevated in this region. Our results suggest that at snowmelt, a complex mixture of chemicals enters aquatic ecosystems that could impact biological communities of the oil sands region.

Introduction

The oil sands of Northern Alberta and Saskatchewan make up 97% of Canada's and one third of the world's proven oil reserves (*1*). Oil sands production is growing and is an important economic driver both nationally and globally, with Canada currently the largest supplier of crude oil and petroleum products to the United States. Growth rates have been rapid, with total oil sands production only 100 000 barrels of oil per day^{-1} (b d^{-1}) in 1980, 1 600 000 b d^{-1} in 2011, and a projected tripling to 4 200 000 b d^{-1} by 2025 (*2, 3*). Monitoring has been carried out to quantify the potential environmental impacts of such rapid resource development in the Athabasca oil sands region. However, several independent expert review panels recently concluded that the largest program, the Regional Aquatic Monitoring Program lacked leadership and, due largely to deficient scientific design and a lack of pre-impact data, were unable to definitively distinguish oil sands industrial impacts (*4, 5, 6, 7*).

In terms of atmospheric contaminant emissions alone, there are concerns regarding bitumen upgrading facilities, vehicle emissions, volatilization from tailings ponds, and blowing dusts from open pit mines, exposed coke piles, and deforested areas (*6*). While atmospheric emissions of several metals and polyaromatic hydrocarbons (PAHs) from oil sands operations have been reported to the National Pollutant Release Inventory (NPRI) since the early 2000s (*8*), it is only recently that deposition of these contaminants has been studied. Kelly et al (*9, 10*) demonstrated that atmospheric deposition of PAHs and the 13 metals considered priority pollutant elements (PPEs) under the US Environmental Protection Agency's Clean Water Act were elevated in snowpacks collected within 50 km of the major bitumen upgrading facilities and other oil sands development (*9, 10*). Dated lake sediment cores have also been used to reconstruct historical PAH loadings to aquatic ecosystems and assess atmospheric sources (*11, 12, 13*). Results demonstrated that PAH deposition has increased by ~2.5-23 times since the ~1960s with increasing alkylated PAHs and dibenzothiophenes, as well as their diagnostic ratios, pointing to an increasingly larger input of petrogenic PAHs coincident with bitumen resource development (*12, 13*).

Of the numerous other contaminants of concern in this region, mercury (Hg), which in addition to being one of the 13 PPEs, is particularly contentious as there are fish consumption advisories for Athabasca River walleye downstream of Fort McMurray (*14*) and consumption of local fishes and birds

is an important aspect of the traditional way of life in this region. Studies have examined trends in fish Hg levels (*15, 16*) with the most recent and comprehensive compilation of available fish Hg data for water bodies of the region finding no clear changes over time for various fish species (*16*). Hg concentrations in gull and tern eggs from the Peace Athabasca Delta (PAD), located ~200 km north of many of the major oil sands developments, have been examined with results suggesting that Hg concentrations increased between 1977 and 2012 in one gull colony, likely due to both local and regional factors (*17*). However, all studies suggested that current datasets do not have sufficient statistical power to definitively detect temporal changes in wildlife Hg levels and that improved experimental design, including consistency in monitoring species and sites and increased sampling size and frequency, are needed if monitoring programs are to conclusively identify trends.

In addition to short-comings in experimental design, the failure to identify consistent temporal changes in biota also reflects the complexity of Hg cycling in the environment. Because gaseous elemental Hg(0) can undergo long-range transport, both local and distant sources contribute to atmospheric deposition of inorganic Hg(II), which is produced by atmospheric oxidation of Hg(0) and is rapidly deposited to landscapes and waterbodies (*18, 19, 20*). For instance, source attribution modelling suggests that ~10-15% of the Hg deposited to the Canadian Arctic originates from east Asia (*21, 22*). Once deposited, Hg(II) undergoes a number of biogeochemical transformations, which dictate its ultimate fate and ability to bioaccumulate. One key process is the microbial methylation of Hg(II) to the toxic bioaccumulative form, methylmercury (MeHg) which primarily occurs under reducing conditions in lakes and wetlands (*23, 24, 25, 20*). Hg(II) and possibly MeHg, may be also emitted directly to the atmosphere from local point sources, such as industrial developments, and then deposited to nearby ecosystems. In fact, spring-time snowpack measurements at ~30 sites located within ~200 km of major oil sands developments on the Athabasca River and tributaries, demonstrated that total Hg (THg; all forms of Hg in a sample) deposition is elevated within 50 km of site AR6, which is located in the heart of the major development area and adjacent to the two major bitumen upgrading facilities (*10*). Here, we also sampled the snowpack, which represents a temporally integrated measure of atmospheric deposition spanning the time period between first snowfall to sampling, to examine spatial trends in atmospheric Hg deposition to the Athabasca oil sands region. Spring-time sampling of the accumulated snowpack at 80 sites located within ~100 km of the major development area in 2012

provided sufficient spatial coverage to estimate Hg loadings to a ~20 000 km^2 area covering the region of major oil sands developments.

Methods:

Study Design: Snow was sampled from numerous sites located varying distances from the major oil sands developments in spring 2011 and 2012. In 2011, many of the Kelly et al. (*9, 10*) sites were sampled, including 27 sites located 0-231 km from the major development area on the Athabasca River and 6 tributaries (Steepbank, Muskeg, Firebag, Beaver, Tar, and Ells rivers). In 2012, the study was expanded to 89 sites and included the 27 sites from 2011, 53 sites located along 8 transects moving away from the major development area, and 9 sites in the PAD, located ~200 km north of the major oil sands developments (Figure S1). Historical Fort McMurray snowpack accumulation data from Environment Canada's National Climate Data and Information Archive was reviewed to target sample collections for maximum snowpack depth (February 26th - March 3rd in 2011, March 6th - March 10th in 2012 for 80 sites and March 20-21st for the 9 PAD sites).

Sampling and Analysis: Sites were accessed by helicopter or snowmobile and samples collected 50-100 m upwind out of the reach of potential fumes and helicopter downwash. Teflon and stainless steel tools used for the snow collections were acid-washed prior to use in the field, and the standard two person "clean hands, dirty hands" Hg sampling protocol was used to minimize potential contamination (*26*). Snow pits were dug to the bottom of level snowpacks using stainless steel shovels, one side of the snow pit was cleaned using a Teflon scraper, and snow was collected by pushing pre-cleaned 1 L IChem© glass jars into the face of the pit to obtain composite snowpack profiles. 3 1 L glass jars (one for THg analysis, one for MeHg, and one that was later filtered and split into samples for THg and MeHg analysis) were collected at each site. Water chemistry and trace metals samples were also collected at each site using similar methods with the exception that snow was collected into pre-cleaned 13 L high density polypropylene pails. Samples were stored frozen until processing at the Canada Centre for Inland Waters (CCIW). To calculate aerial contaminant loadings, 10 snow cores were collected at each site using an Adirondack corer and the weight of each core was obtained for determination of snow water equivalence (SWE).

Snow samples were melted in the dark in a clean laboratory. Samples for analysis of dissolved THg and MeHg concentrations were filtered through 0.45 µm nitrocellulose membranes in acid washed Nalgene filter units then all Hg samples were preserved with concentrated trace metal grade HCl equal to 0.2% of the sample volume. THg and MeHg concentrations were determined using standard protocols (*27, 28, 29*) at the CCIW Low-Level Analytical Laboratory. Standard water chemistry analysis and 45 multielement scan were carried out at the National Laboratory for Environmental Testing (NLET) in Burlington, ON, Canada. Analytical details are provided in the Supporting Information.

Determination of loadings to the oil sands region: SWE and net loadings were determined for each site as in (*9, 10, 30*). Briefly, SWE was determined as follows:

$$\text{SWE (kg m}^{-2}\text{)} = \text{core weight (kg)}/(\pi(\text{corer radius (m)})^2) \quad (1)$$

Average areal water volumes (L m^{-1}) were then calculated for each site using the below formula:

$$\text{Aerial water volume (L m}^{-2}\text{)} = \text{SWE (kg m}^{-2}\text{)}/\text{density water (kg m}^{-3}\text{)} \times 10^3 \text{ L m}^{-3} \quad (2)$$

then multiplied by average concentrations (ng L^{-1}) of Hg in snow melt to determine springtime loadings of THg (ng m^{-2}) for each site.

2012 spatial coverage on the landscape was sufficient to allow interpolation of spring-time THg and MeHg loadings for ~20 000 km^2 area (56.9997, -110.6657 to 57.0032, -112.4782 and 56.4624, -111.451 to 57.7799, -111.3619) using ArcGIS10© Geostatistical Analyst software (Esri, Redlands, California). All kriging surfaces used a simple prediction and lognormal, gamma, or empirical base distribution. The number of neighbours included in each kriging was based on how closely related neighbouring data points were to each other and ranged from 4-6. Details on the kriging settings for each parameter examined are provided in Table S1.

Results and Discussion

Snowpack characteristics: Snowpacks consisted of a granular depth hoar layer created by temperature gradient metamorphism over the winter, overlain by a denser layer deposited throughout the spring (*31*). Although average snowpack depth varied from site to site (range 9-45 cm; average 29 ± 11 cm),

overall there was a linear relationship between snowpack depth and SWE (r^2 = 0.66, p<0.01), demonstrating that snowpack density was fairly consistent over the sampling region (Figure S2). Snowpacks at some sites within the major development area, such as site AR6 which is located on the Athabasca River and adjacent to the two major bitumen upgraders, had visible dark layers while others appeared fairly white (Figure S3). This layering could result from melt-freeze cycles which caused percolation of particulate matter through the snowpack and formation of dark layers upon refreezing or from large episodic emission/deposition events.

Spatial patterns in Hg deposition to the Alberta oil sands region. Spring-time snowpack THg concentrations ranged from 0.8 to 14.4 ng L^{-1} with lowest concentrations observed in the PAD (n=9, average = 1.19 ± 0.24 ng L^{-1}) as well as at numerous distal sites along our 8 transect lines. Highest THg concentrations (>8 ng L^{-1}) were observed at 15 sites within the major oil sands development area, predominantly in the region between the Muskeg and Steepbank rivers (Figure S4). MeHg concentrations were also elevated in this area, reaching up to 0.27 ng L^{-1} and decreasing to concentrations just at or above the method detection limit of 0.015 ng L^{-1} in the PAD and at several distal sites (average = 0.016 ± 0.002 ng L^{-1} in the PAD). Given that snowpacks provide a direct measure of atmospheric deposition, these results suggest that oil sands developments are a source of airborne THg and MeHg emissions to local landscapes and water bodies. Generally, inorganic Hg(II) that is deposited in precipitation to landscapes and waterbodies and must undergo a methylation step before it can be taken up by organisms and biomagnified through food chains. Therefore, the elevated MeHg levels in snowpacks may be of particular relevance to aquatic and terrestrial ecosystems of the region. The THg and MeHg deposited to snowpacks of the Athabasca oil sands region was predominantly bound to particulates >0.45 µm in size (79 ± 12 and 72 ± 18% particulate-bound, respectively), which may affect its transport, availability for uptake by organisms, and ultimately its impact on local ecosystems.

To determine the quantity of Hg that enters ecosystems at spring snowmelt, springtime snowpack Hg loadings (ng m^{-2}) were calculated using snowpack Hg concentrations (ng L^{-1}) and average snow water equivalence (L m^{-2}). Similar to Hg concentrations, THg and MeHg loadings were elevated at many sites within the major development area, reaching up to 1420 and 19 ng m^{-2}, respectively, and

decreasing to 103 ± 42 and 1.2 ± 0.2 ng m^{-2}, respectively, in the PAD (Figure 1 and S5). Due to increased sampling intensity in 2012, we were able to explore deposition patterns on the landscape by interpolating measured Hg loadings using ArcGIS geostatistical software for a ~20 000 km^2 area surrounding the current oil sands developments (Figures 1 and S5). The kriged interpolations produced deposition maps with areas of maximum THg and MeHg loadings located primarily between the Muskeg and Steepbank rivers and resembling a bullseye pattern on the landscape. This deposition pattern was consistent for numerous other parameters examined, including metals known to be emitted in large quantities from the upgrading facilities (e.g., Ni, V, and Zn), crustal elements (Al and La), and total suspended solids (TSS) (see below and Figure S6 for deposition maps of V, Al, and TSS). Patterns in particulate-bound Hg deposition were similar, whereas dissolved THg and MeHg deposition was fairly low over the entire region (<200 and 3 ng m^{-2}, respectively) (Figures S5). The deposition maps were used to estimate the area (km^2) receiving different loadings and suggested that ~227 and 133 km^2, respectively, received maximum THg and MeHg loadings of >600 and 12 ng m^{-2}, respectively (Table S2).

Kelly et al. (*9, 10*) used distance from site AR6, to examine spatial patterns in contaminant deposition to this region. The deposition maps produced from our measured Hg loads suggest that in 2012, the region of maximum deposition was centred <20km from site AR6. Therefore, similar to Kelly et al. (*10*), plotting measured Hg loadings versus distance from AR6 produced a roughly exponential decay relationship (Figure 2). Because kriging averages measured loads at neighbouring sites to create contours, and measured THg and MeHg loads varied along small spatial scales within the major development area (by up to 68% among sites located <5km from each other), some measured Hg loadings fell out of the kriged loading areas. To test if kriged interpolations significantly over- or under-estimated contaminant deposition to the oil sands region, mean measured loadings were compared to kriged means within each kriged area using paired t-tests (Table S3). No significant differences were found ($p>0.05$, Table S3), demonstrating that overall, the kriging parameters used resulted in an appropriate fit of measured deposition. The deposition maps (Figure 1 and S5) capture regional patterns in Hg deposition, but may be unable to resolve variation on local scales, possibly due to the presence of multiple sources of varying magnitude. To improve future deposition mapping, snowpack

sampling should be performed along a grid-work at sufficient frequency to capture variation along both local and regional scales.

Although it is difficult to estimate loadings un-impacted by oil sands developments in the absence of long-term monitoring data, THg and MeHg deposition at our most distant sites in the PAD, which is located ~150-200 km north of the major developments and has no major Hg point sources, averaged only 103 ± 42 and 1.2 ± 0.2 ng m^{-2}, respectively (n = 9). These baseline values compare well to those observed using the flat portion of the exponential decay curved obtained from plotting THg and MeHg loads versus distance from AR6 (Figure 2). Assuming that <100 and 1.5 ng m^{-2} represent respective THg and MeHg loadings un-impacted by oil sands developments, our results suggest that almost the entire ~20, 000 km^2 sampling area where spatial coverage was sufficient to allow interpolation of Hg loadings is currently impacted by airborne Hg emissions originating in the oil sands development area. In fact, at the most distal sites sampled to the east and northeast of AR6 (E-S9 and NE-S10, which are located 50 km from AR6), THg and MeHg loadings were >200 and 5 ng m^{-2}, respectively, which are well above the observed baseline values. Future sampling will therefore include numerous sites located further away from the major development area. Using average particulate-bound THg loads of 56 ± 33 ng m^{-2} in the PAD to represent baseline values, we estimate that ~16 800 km^2 is impacted by oil sands-associated particulate-bound Hg emissions. Although dissolved THg loadings were elevated (up to 111 ng m^{-2}) at some sites within the major development area, loadings were generally low over the entire sampling region (average 45 ± 17 versus 47 ± 15 ng m^{-2} at sites in the Athabasca oil sands region compared to in the PAD) making it impossible to determine the size of the area impacted by dissolved THg emissions and suggesting that dissolved Hg emissions are either minimal from oil sands operations, or that dissolved Hg and Hg bound to fine particulates undergo long range transport. Only unfiltered MeHg samples were obtained from the PAD making it difficult to define baseline particulate-bound MeHg loadings for the oil sands region; however we hypothesize that the footprint is similar to that observed for THg.

Although our results suggest that Hg deposition is elevated above baseline for an area of ~20, 000 km^2, both the deposition maps and plots of loadings versus the distance from AR6 suggest that Hg loads decrease fairly rapidly from maximum depositional zones. For example, for THg and MeHg, 89 and 80%, respectively, of the ~20 000 km^2 area examined receive loads <half those observed in the

maximum deposition zone (<300 and 6 ng m^{-2}, respectively). Similarly, plots of Hg loads versus distance from AR6 suggest that deposition decreases dramatically at ~50 km from AR6 (Figure 2). Using interpolated loading, we therefore calculated the quantity of Hg deposited to the area within a 50 km radius of AR6. We estimate that ~1.9 and 0.05 kg of THg and MeHg, respectively, were deposited to the landscape within a 50 km of AR6 during the ~4 month period between the first major snowfall and sampling in the spring (November 15th, 2011 to March 6-10th, 2012) (Table 1). 52 kg of airborne Hg emissions was reported to NPRI (*8*) from Athabasca oil sands industries in 2011 and 2012. Assuming that airborne emissions do not vary greatly from month to month, 17 kg of THg was emitted over the ~4 months of winter 2012, which suggests that a large percentage of Hg emitted from oil sands operations is transported further than 50 km from AR6 or that a portion of the Hg deposited within 50 km of AR6 is lost post-deposition.

Comparison of mercury loadings to previous work. The patterns and magnitude in THg deposition reported here are similar to those reported by Kelly et al. (*10*) for winter 2008 (Figure 2). For example, particulate-bound THg at the same 19 sites located <50 km from AR6 averaged 268, 232, and 307 ng m^{-2} in 2008, 2011, and 2012, respectively. In fact, measured THg and MeHg loadings did not differ significantly among 2011 and 2012 at the 25 sites sampled in both years (paired t-test, p=0.30 and 0.12, respectively (Figure S7)). There is one other published study on atmospheric Hg deposition to this region, which utilized both Hg concentrations and Hg stable isotope composition in epiphytic tree lichen *H. physodes* to examine spatial trends in Hg deposition within ~150 km of the major mines and processing locations (*32*). Although concentrations of some metals (Al and V) did increase in *H. physodes* with proximity to the major developments (*33*), Hg concentrations did not follow this trend and actually decreased within 25 km of the major developments, which the authors attributed to physiological responses of the lichen to enhanced SO_2 deposition (*32*). Concentrations of atmospheric total gaseous Hg(0) (TGM) were measured near Fort McMurray from 2010-2012 and were found to be driven predominantly by long-range transport (*34*). However, our snowpack measurements suggest that the locations of the TGM measurements fell out of the region of elevated Hg deposition. Furthermore, the monitoring did not include atmospheric measurements of particulate-bound THg or MeHg, which are likely of concern in this region.

Spring-time snowpack sampling has been used to quantify Hg loadings at the Experimental Lakes Area (ELA), located in a remote region of northwestern Ontario, Canada, for the last 10 years. Because THg and MeHg loadings varied greatly from site-to-site within the major oil sands development area, average winter-time loadings within 50 km of AR6 (354 ± 284 and 7 ± 4 ng m^{-2}, respectively) were only slightly higher than those observed at the ELA (average 280 ± 175 and 6 ± 3 ng m^{-2}, respectively from 1992-2010) (*35*). Furthermore, although Hg loadings within the major development area are clearly elevated above background levels for this region, maximum THg loadings are low compared to those in contaminated regions of the northern hemisphere directly influenced by numerous anthropogenic sources, such as parts of the eastern United States, western Russia, Japan, Korea, and China where winter-time loadings can reach >20,000 ng m^{-2} (*36*).

What are the factors driving spatial trends in Hg deposition? Relationships between Hg and numerous parameters, including natural environmental factors such as snowpack characteristics and wind, as well as other chemicals, were examined to identify potential factors driving the spatial patterns in Hg deposition to the oil sands region. Concentrations and loadings of THg and MeHg and the other parameters examined were not normally distributed (Shapiro-Wilk normality test, $p<0.05$) and were thus log transformed prior to statistical analyses. Multiple linear regression modeling demonstrated that Hg loadings were driven primarily by Hg concentration rather than by snowpack depth or snow water equivalence, with concentrations explaining 78 and 82% of the variability in THg and MeHg loadings, respectively (Table S4). These results suggest that local Hg emissions, and not precipitation quantity, drive Hg deposition to snowpacks in the oil sands region.

Distance from AR6 explained 41 and 48% ($p<0.01$) of the variation in THg and MeHg loadings, respectively, suggesting that there are additional sources of atmospheric Hg emissions besides the upgraders near AR6, or that wind patterns affect the distribution of local Hg emissions. Predominant winds in the Alberta oil sands region are generally from the east, southwest and northwest (Table S5, Figure S8). For example, during the period spanning first snowfall in 2011, to the time of snow sampling in 2012, the wind direction was from the east, southwest, and northwest 22, 20 and 20% of the time, respectively, and from the north, northeast and south only 7, 5, and 3% of the time, respectively. However, wind direction alone explained only a minor portion of the variation in Hg loads

and was not statistically significant for MeHg (r^2 = 0.20 and 0.14, p = 0.01 and 0.07, respectively) (Table S4). In fact, although winds blew from the east to the west with the greatest frequency throughout winter 2012 (22% of the time), THg loadings at sites to the west of AR6 were significantly lower than those at sites to the north, northeast, and east of AR6 (Bonferonni and Tukey's post-hoc comparisons, p<0.03). Wind speed was also examined and varied significantly with wind direction (ANOVA followed by post-hoc comparisons; p<0.03); however, together wind speed, wind direction, and distance from AR6 explained an additional 15% of the variation in Hg loads than distance from AR6 alone (ANCOVA; r^2=0.56 and 0.63, p < 0.01; Table S4). Given that the majority of the THg and MeHg in snowpacks of the oil sands region was particulate-bound, we hypothesize that particulate-bound emissions to the atmosphere are rapidly deposited near local point sources.

Relationships between Hg and numerous elements and water chemistry parameters were explored to see if chemical signatures characteristic of similar emission sources could be identified. TSS explained a large proportion of the variability in THg and MeHg concentrations (r = 0.85 and 0.80, respectively, p<0.01; Table S6 and Figure S9). Kelly et al. (*9*) also reported high loadings of airborne particulates to snowpacks of the oil sands region and by extrapolation of the observed exponential relationship between TSS loadings and distance from, they estimated that 11, 400 metric T of suspended solids was deposited to the area within 50 km of AR6 over winter 2008. Using a geostatistical approach, which likely captured the spatial heterogeneity in contaminant deposition more accurately, we estimate a 2012 winter-time TSS loading of ~25 800 T, (Table 1).

Concentrations of THg and MeHg were also significantly correlated with numerous metals. For example, vanadium (V), Zn, and Ni, all of which are known to be emitted in large quantities from oil sands operations, explained a large proportion of the variation in THg and MeHg concentrations (r = 0.73-0.86, p<0.01) (Table S6 and S7). In 2011, 12, 384 kg of airborne metals emissions was reported to NPRI (*8*), of which V, Zn and Ni together comprised 85% (5048, 2957, 2444 kg of V, Zn and Ni respectively) (Table 1 and S7). Interpolation of measured V, Zn, and Ni loadings for the area within 50 km of AR6 produced deposition estimates of 3000, 8560, and 1460 kg, respectively, for winter 2012. Assuming that airborne emissions do not vary greatly among seasons, comparison of emissions data with winter-time loadings for the region within 50 km of AR6 suggests that the airborne emissions reported to NPRI are underestimated, especially for Zn (Table 1). This is consistent with a recent

322 modeling study that suggested that oil sands industry PAHs emissions are underestimated by up to two
323 orders of magnitude (*37, 38*).
324
325 Significant relationships were also observed between THg and MeHg and crustal elements
326 aluminum (Al), iron (Fe), and lanthanum (La) (Table S6), suggesting similar source signatures or
327 transport pathways among these elements, although airborne emissions estimates are not available on
328 the NPRI website for these elements (*8*). Correlation coefficients between TSS, Ni, V, Zn and Ni, Pb, TSS,
329 and Al, Fe and La ($r = 0.79\text{-}0.99$, $p < 0.01$), were consistently higher than between these parameters and
330 THg and MeHg, suggesting that THg and MeHg undergo post-depositional processing in snowpacks,
331 likely by photoreduction and photodemethylation, respectively. In Arctic surface snow, the lifetime of
332 Hg(II) has been estimated at ~16 days (*39*) with losses of ~35-50% observed within 10.5 hrs of light
333 exposure (*40*); although photoreduction rates are known to vary depending on snowpack chemistry
334 and characteristics (*41*). Rates of snowpack MeHg photodegradation have not been quantified;
335 however in Canadian freshwater ecosystems, photodemethylation is an important mechanism for
336 removing MeHg from surface waters with rates averaging 3.8 to 11.3 X 10^{-3} hr^{-1} (*42, 43; 44*). Thus, the
337 THg and MeHg loadings presented here represent *net* spring-time loadings rather than *gross*
338 deposition from local emission sources.
339 Despite potentially different post-depositional processing of individual metals in snowpacks,
340 deposition maps for Hg, metals known to be emitted in large quantities from the upgrading facilities,
341 crustal elements, and TSS, demonstrated a remarkably similar bullseye pattern in contaminant
342 deposition, with areas of maximum loading located predominantly between the Muskeg and
343 Steepbank rivers (Figure S6 for example). Graney et al. (*32*) produced contoured maps of V and Al
344 concentrations in lichen *H. physodes* from 2008 lichen samples collected from 121 sites within ~150 km
345 of the major developments using graphical contouring program Surfer. They observed a similar
346 bullseye pattern in lichen V and Al concentrations, which are indicative of long-term deposition
347 patterns but cannot be translated to depositional fluxes or loadings.
348 Of the water chemistry parameters examined, Hg was significantly related to total phosphorous
349 (TP), particulate organic carbon (POC), and particulate organic nitrogen (PON) ($r = 0.74\text{-}0.82$, $p<0.01$),
350 which were also deposited in large quantities within the development area (Table 1 and S6). Due to the

important role of DOC in controlling the transport of THg and MeHg as well as rates of Hg(II) methylation to MeHg in aquatic ecosystems, Hg and DOC are often tightly correlated in lakes and rivers (*20, 43, 25, 46*). Significant relationships between Hg and sulfate are also often observed as sulfate can control Hg(II) speciation and Hg(II) methylation rates by sulfate reducing bacteria, which are often the principal methylating bacteria present in aquatic ecosystems (*47, 48*). Sulfate and DOC deposition was elevated in snowpacks of the Athabasca oil sands region. However, correlation coefficients between both THg and MeHg and DOC and sulfate were lower ($r = 0.45$-0.54, $p<0.01$) compared to those observed between the metals and other water chemistry parameters examined. These results indicate that there are different sources or transport pathways for dissolved and particulate-bound substances emitted from various oil sands-related processes. Receptor modeling using an inventory of inorganic contaminants in materials from different stages of the oil sands production cycle and the 2008 lichen dataset described above (*32*) suggested that the sources impacting lichen contaminant concentrations were: oil sand and processed material, tailing sand fugitive dust, combustion processes, limestone and haul road fugitive dust and a general urban source (*49*). Pb isotopes ratios were also examined and may be a promising tool for source attribution in snow and other environmental media, such as sediment (*32*).

Potential sources of MeHg to snowpacks of the oil sands region. MeHg may be produced *in situ* in snowpacks by the methylation of deposited Hg(II). However, all current proposed mechanisms are specific to Arctic coastal snowpacks and therefore invoke the presence of marine air masses or sea spray for MeHg production (*50, 51, 52*). For example, transmethylation reactions involved in the degradation of dimethylsulfoniopropionate (DMSP), an organosulfur compound produced by marine phytoplankton, were recently implicated to explain high MeHg concentrations in Svalbard snowpacks (*451, 53*). Hg(II) methylation in precipitation prior to deposition is also possible. Based on a strong correlation between MeHg and reactive Hg(II) (a fraction of Hg that includes mostly labile Hg(II) complexes) in precipitation samples from across North America, it was hypothesized that MeHg in precipitation is formed predominantly by aqueous phase methylation in the atmosphere (*54*). However, to produce the almost identical bullseye patterns in THg and MeHg deposition for winter 2012, methylation rates would need to be consistent over the entire region examined. This seems

unlikely, since methylation rates are a function of both the quantity of bioavailable Hg(II) present in the environment and the activity of microorganisms carrying out Hg(II) methylation (*55*), which in turn is dependent on energy sources for microbes and redox conditions. Furthermore, the %MeHg, which is an indicator of active methylation in aquatic ecosystems (*56, 57*), was quite low (average 2.5 ± 1.7% in 2012), and varied from site to site throughout the entire sampling region. Finally, the positive significant relationships observed between MeHg and other contaminants known to be emitted from oil sands related processes (for example, V, Zn, and Ni) suggests that MeHg is also released directly to the atmosphere from industrial processes. Measurement of MeHg from various potential emission sources is therefore warranted. Examination of Hg transformations in snowpacks, including potential rates of Hg(II) methylation, using amendments of snowpacks with enriched Hg stable isotope tracers as has been carried out in lake waters (*58*) would also be informative.

Relevance to Ecosystems of the Athabasca oil sands region: Chemicals in snowpacks enter terrestrial and aquatic ecosystems at spring snow melt where they may impact biological communities. At all sites examined, concentrations of THg and MeHg in melted snow were below the Canadian Council of Ministers of the Environment (CCME) guidelines for the Protection of Aquatic Life of 26 and 4 ng L^{-1}, respectively (*59*; Table S8). Of the other metals examined, CCME guidelines were not exceeded for Ni but were exceeded at a number of the 89 sites in 2012 for Pb, Zn, Fe, and Al (21 for Pb, 3 for Zn, 54 for Fe and 76 for Al) (Table S8). Interestingly, because the CCME guideline for Al is pH dependent (the Al threshold drops from 100 to 5 µg L^{-1} for snow of pH <6.5) and the snow was acidic and many of our sites (6.2 ± 1.2; range 1.6 to 8.4), the guideline for Al was exceeded at 8 of the 9 distal sites in the PAD. CCME guidelines are not currently available for V and La, which were also elevated in snowpacks within the major development area (Figure S6). TP is also deposited to snowpacks in the Athabasca oil sands region (Table 1), with melted snow considered eutrophic (35-100 µg L^{-1}) or hyper-eutrophic (>100 µg L^{-1}) at 40 sites according to CCME guidelines (Table S8). Although comparison of snowmelt concentrations to CCME or other guidelines allows concentrations to be placed into context, a number of complex processes control the exposure of organisms to chemicals entering ecosystems. For example, the impact of snowpack loads on chemical concentrations in aquatic ecosystems depends on the processes controlling delivery to lakes and rivers and post-delivery mixing processes. Recent

409 analysis of 38 years (1978-2010) of water quality data for 7 rivers draining the oil sands region,
410 suggests that concentrations of several metals (for example, As, uranium and V) increased coincident
411 with periods of major development, including open-pit mining and SAGD (Steam Assisted Gravity
412 Drainage) (*60*). Further work linking snowpack loadings to hydrology is therefore needed to determine
413 the relative importance of atmospheric deposition in driving observed trends in river water
414 contaminant concentrations. Finally, the impacts of complex chemical mixtures, including
415 contaminants such as Hg, on aquatic and terrestrial ecosystems are also dependent on the ecological
416 processes controlling rates of contaminant bioaccumulation and biomagnification through food webs;
417 therefore detailed food web studies which track the uptake of contaminants and effects on the health
418 of biological communities is needed.
419
420 **Figure Captions**
421
422 Figure 1. Deposition of THg and MeHg to the Athabasca Oil Sands region in winter 2012. Interpolated
423 THg and MeHg loads (ng m^{-2}) produced using ArcGIS Geostatistical Analyst software are overlain by
424 measured loads (ng m^{-2}) at each site.
425
426 Figure 2. Winter 2011 and 2012 loadings (ng m^{-2}) of unfiltered THg (A) and MeHg (C), particulate-bound
427 THg (B) and MeHg (D) versus distance from site AR6 in the Athabasca Oil Sands region. Particulate-
428 bound THg and MeHg concentrations were calculated by the difference between unfiltered and
429 filtered samples.
430
431 **Acknowledgements**
432 We thank Environment Canada and the Joint Oil Sands Monitoring Program for funding. We thank
433 Research and Support Services at the Canada Centre for Inland Waters and the following individuals for
434 sample collections and laboratory analysis: Jonathan Keating, Charlie Talbot, Carolyn Tunks, Rodney
435 McInnis, Janna Coty, Amy Sett, Mark Duric, Carl Yanch, Xiaowa Wang, Greg Lawson, and Alyyah
436 Thawer. We would also like to everyone at Wood Buffalo Helicopters for their assistance with sample
437 collections, especially Mike Morin and Cory Leahy. Emily Pallard of Strategic Forest Management made

Figures 2, and S1, S4, S5 and S6 and provided GIS support. Finally, we are grateful for our collaboration with Bruce Maclean and the Mikisew Cree First Nation of Fort Chipewyan which resulted in snow collections in the Peace Athabasca Delta.

Supporting Information Available

Analytical details, eight tables, and eight figures are available in the supporting information. This information is available free of charge via the Internet at http://pubs.acs.org/.

Table 1. Winter 2012 loads of THg, MeHg, total suspended solids (TSS), total phosphorous (TP), total nitrogen (TN), particulate organic nitrogen (PON), vanadium (V), zinc, nickel (Ni), aluminum (Al), and iron (Fe) to landscapes and water bodies within 50 km of AR6 as well as oil sands industry airborne metals emissions as reported to the National Pollutant Release Inventory for the Athabasca oil sands region for 2011 and 2012 (*7*).

Contaminant	**Winter 2011-2012 loads within 50 km AR6**	**Annual 2011 airborne emissions as reported to NPRI**	**Annual 2012 airborne emissions as reported to NPRI**	**Estimated 2012 winter emissions[1]**
	(kg or T*)	**(kg)**	**(kg)**	**(kg)**
THg	1.9	52	52	16
MeHg	0.05			
TSS	25 890*			
TP	28.6*			
TN	463*			
PON	153*			
V	3000	5048	5140	1594
Zn	8560	2957	3492	1022
Ni	1470	2444	2962	858
Al	793*			
Fe	2150*			

[1]Winter 2012 emissions were estimated by weighting annual emissions for the number between the first snowfall (November 15th, 2011) and snowpack sampling (March 7th, 2012; n= 47 and 67 days in 2011 and 2012, respectively).

*refers to metric Tonnes

References

1. *OPEC Annual Statistical Bulletin 2010/2011*. OPEC (Organization of the Petroleum Exporting Countries): Vienna, 2011; www.opec.org/opec_web/en/publications/202.htm.
2. Stringham, G. Energy developments in Canada's oil sands. In *Alberta Oil Sands: Energy, Industry and the Environment*; Percy, K. E., Eds.; Elsevier: Kidlington, Oxford 2012**;** pp 19-34.
3. *Canadian Crude Oil Production Forecast 2012-2013*. CAPP (Canadian Association of Petroleum Producers): Calgary, 2012, http://www.capp.ca/forecast.
4. *Regional Aquatic Monitoring Program (RAMP) Scientific Review*. Alberta Innovates Technology Futures: Calgary, 2011; http://www.ramp-alberta.org/ramp/news.aspx.
5. *Environmental and Health Impacts of Canada's Oil Sands Industry*. The Royal Society of Canada: Ottawa, 2010; https://rsc-src.ca/en/expert-panels/rsc-reports/environmental-and-health-impacts-canadas-oil-sands-industry.
6. *A Foundation for the future: Building an environmental monitoring system for the oil sands*. *A report submitted to the Minister of the Environment*; Environment Canada: Gatineau, Canada, 2010; https://www.ec.gc.ca/pollution/default.asp?lang=En&n=EACB8951-1.
7. Dillion, P.; Dixon, G.; Driscoll, C.; Giesy, J.; Hurlbert, S.; Nriagu, J. Evaluation of four reports on contamination of the Athabasca River system by oil sands operations. *A report prepared for the Government of Alberta*, 2011.
8. The National Pollutant Release Inventory (NPRI); http://ec.gc.ca/inrp-npri/.
9. Kelly, E. N.; Short, J. W.; Schindler, D. W.; Hodson, P. V.; Ma, M.; Kwan, A. K.; Fortin, B. L. Oil sands development contributes polycyclic aromatic compounds to the Athabasca River and its tributaries. *PNAS.* **2009**, *106*, 22346-22351.
10. Kelly, E. N.; Schindler, D. W.; Hodson, P. V.; Short, J. W.; Radmanovich, R.; Nielson, C. C. Oil sands development contributes elements toxic at low concentrations to the Athabasca River and its tributaries. *PNAS.* **2010***, 107*, 16178-16183.
11. Hall, R. I.; Wolfe, B. B; Wiklund, J. A.; Edwards, T. W. D.; Farwell, A. J.; Dixon, D. G. Has Alberta oil sands development altered delivery of polycyclic aromatic compounds to the peace-athabasca delta?. *PloS one* 7. **2012**, *9*, e46089.

12. Kurek, J.; Kirk, J. L.; Muir, D. C. G.; Wang, X.; Evans, M. S.; Smol, J. P. The legacy of a half century of Athabasca oil sands development recorded by lake ecosystems. *PNAS.* **2013**, *110*, 1761-1766.
13. Jautzy, J.; Ahad, J. M. E.; Gobeil, C.; Savard, M. M. Century-long source apportionment of PAHs in Athabasca oil sands region lakes using diagnostic ratios and compound-specific carbon isotope signatures. *Environ. Sci. Technol*. **2013**, *47*, 6155-6163.
14. MywildAlberta.com-fishconsumptionadvisory; http://mywildalberta.com/Fishing/SafetyProcedures/FishConsumptionAdvisory.aspx.
15. Timoney, K. P.; Lee P. Does the Alberta tar sands industry pollute? The scientific evidence. *Open Conserv. Biol. J*. **2009**, *3*, 65-81.
16. Evans, M.; Talbot, A. Investigations of mercury concentrations in walleye and other fish in the Athabasca River ecosystem with increasing oil sands developments. *J. Environ. Monit*. **2012**, *14*, 1989-2003.
17. Hebert, C. E.; Campbell, D.; Kindopp, R.; MacMillan, S.; Martin, P.; Neugebauer, E.; Patterson, L.; Shatford, J. Mercury trends in colonial waterbird eggs downstream of the oil sands region of Alberta, Canada. *Environ. Sci. Technol.* **2013**, *47*, 11785-11792.
18. Schroeder, W. H.; Munthe, J. Atmospheric mercury-an overview. *Atmos. Environ.* **1998**, *32*, 809-822.
19. Pirrone, N.; Cinnirella, S.; Feng, X.; Finkelman, R. B.; Friedli, H. R.; Leaner, J.; Mason, R.; Stracher, G. B.; Streets, D. G.; Telmer, K. Global mercury emissions to the atmosphere from anthropogenic and natural sources. *Atmos. Chem. Phys*. **2010**, *10*, 5951-5964.
20. Driscoll, C. T.; Mason, R. P.; Chan, H. M.; Jacob, D. J.; Pirrone, N. Mercury as a global pollutant: sources, pathways, and effects. *Environ. Sci. Technol.* **2013**, *47*, 4967-4983.
21. Durnford, D.; Dastoor, A.; Figueras-Nieto, D.; Ryjkov, A. Long range transport of mercury to the Arctic and across Canada. *Atmos. Chem. Phys. Disc*. **2010**, *10*, 4673-4717.
22. AMAP, 2011. AMAP Assessment 2011: Mercury in the Arctic. Arctic Monitoring and Assessment Programme (AMAP), Oslo, Norway. xiv + 193 pp.
23. Gilmour, C. C.; Henry, E. A.; Mitchell, R. Sulfate stimulation of mercury methylation in fresh-water sediments. *Environ. Sci. Technol.* **1992**, *26*, 2281-2287.

24. Benoit, J. M.; Gilmour, C. C.; Heyes, A.; Mason, R. P.; Miller, C. L. Geochemical and biological controls over methylmercury production and degradation in aquatic ecosystems, In *Biogeochemistry of Environmentally Important Trace Elements*; Chai, Y., Braids, O. C., Eds.; American Chemical Society: Washington, D.C. 2003; pp 262-297.
25. Ullrich, S. M.; Tanton, T. W.; Abdrashitova, S. A. Mercury in the aquatic environment: A review of factors affecting methylation. *Crit. Rev. Environ. Sci. Technol.* **2001**, *31***,** 241-293.
26. St. Louis, V. L.; Rudd, J. W. M.; Kelly, C. A.; Beaty, K. G.; Bloom, N. S.; Flett, R. J. Importance of wetlands as sources of methyl mercury to boreal forest ecosystems. *Can. J. Fish. Aquat. Sci.* **1994**, *51*, 1065-1076.
27. Bloom, N. S.; Crecelius, E. A. Determination of mercury in seawater at subnanogram per liter levels. *Mar. Chem.* **1983**, *14*, 49-59.
28. Bloom, N. S. Determination of picogram levels of methylmercury by aqueous phase ethylation, followed by cryogenic gas chromatography with cold vapour atomic flourescence detection. *Can. J. Fish. Aquat. Sci.* **1989**, *46*, 1131-1140.
29. Horvat, M.; Bloom, N. S.; Liang, L. Comparison of distillation with other current isolation methods for the determination of methyl mercury compounds in low level environmental samples. Part II. *Water. Anal. Chim. Acta*. **1993**, *281*, 135-152.
30. Kirk, J. L.; St. Louis, V. L.; Sharp, M. J. Rapid reduction and re-emission of mercury deposited into snowpacks during atmospheric mercury depletion events at Churchill, Manitoba, Canada. *Environ. Sci. Technol.* **2006**, *40*, 7590-7596.
31. Sharp, M.; Skidmore, M.; Nienow, P. Seasonal and spatial variations in the chemistry of a high Arctic supraglacial snowcover. *J. Glaciol*. **2002**, *48*, 149-158.
32. Blum, J. D.; Johnson, M. W.; Gleason, J. D.; Demers, J. D.; Landis, M. S.; Krupa, S. Mercury concentration and isotopic composition of epiphytic tree lichens in the Athabasca oil sands region. In *Alberta Oil Sands: Energy, Industry and the Environment*; Percy, K. E., Eds.; Elsevier: Kidlington, Oxford 2012**;** pp 373-390.
33. Graney, J. R.; Landis, M. S.; Krupa, S. Coupling lead Isotopes and element concentrations in epiphytic lichens to track sources of air emissions in the Athabasca oil sands region. In *Alberta*

Oil Sands: Energy, Industry and the Environment; Percy, K. E., Eds.; Elsevier: Kidlington, Oxford 2012**;** pp 343-372.

34. Parsons, M. T.; McLennan, D.; Lapalme, M.; Mooney, C.; Watt, C.; Mintz, R. Total gaseous mercury concentration measurements at Fort McMurray, Alberta, Canada. *Atmosphere* **2013**, *4*, 472-493.
35. Graydon, J. A.; St. Louis, V. L.; Hintelmann, H.; Lindberg, S. E.; Sandilands, K. A.; Rudd, J. W.; Kelly, C. A.; Hall, B. D.; Mowat, L. D. Long-term wet and dry deposition of total and methyl mercury in the remote boreal ecoregion of Canada. *Environ. Sci. Technol*. **2008**, *42*, 8345-8351.
36. Durnford, D.; Dastoor, A.; Ryzhkov, A.; Poissant, L.; Pilote, M.; Figueras-Nieto, D. How relevant is the deposition of mercury onto snowpacks?-Part 2: A modeling study. *Atmos. Chem. Phys.* **2012**, *19*, 9251-9274.
37. Parajulee, A; Wania, F. Evaluating officially reported polycyclic aromatic hydrocarbon emissions in the Athabasca oil sands region with multimedia fate model. *PNAS* **2014**, *111*, 3344-3349.
38. Shindler, DW. Unravelling the complexity of pollution by the oil sands industry. *PNAS* **2014**, *111*, 3209-3210.
39. Brooks, S.; Arimoto, R.; Lindberg, S.; Southworth, G. Antarctic polar plateau snow surface conversion of deposited oxidized mercury to gaseous elemental mercury with fractional long-term burial. *Atmos. Environ.* **2008**, *42*, 2877-2884.
40. Sherman, L. S.; Blum, J. D.; Johnson, K. P.; Keeler, G. J.; Barres, J. A.; Douglas, T. A. Mass-independent fractionation of mercury isotopes in Arctic snow driven by sunlight. *Nat. Geosci.* **2010**, *3*, 173-177.
41. Durnford, D.; Dastoor, A. The behavior of mercury in the cryosphere: a review of what we know from observations. *J. Geophys. Res.* **2011**, *116,* D06305*.*
42. Sellers, P.; Kelly, C. A.; Rudd, J. W. M. Fluxes of methylmercury to the water column of a drainage lake: the relative importance of internal and external sources. *Limnol. Oceanogr.* **2001**, *46***,** 632-631.
43. Lehnherr, I.; St. Louis, V. L. Importance of ultraviolet radiation in the photodemethylation of methylmercury in freshwater ecosystems. *Environ. Sci. Technol.* **2009**, *43*, 5692-5698.

592 44. Lehnherr, I.; St. Louis, V. L.; Emmerton, C. A.; Barker, J. D.; Kirk, J. L. Methylmercury cycling in
593 high Arctic wetland ponds: Sources and sinks. *Environ. Sci. Technol.* **2012**, *46*, 10514-10522.
594 45. Dittman, J. A.; Shanley, J. B.; Driscoll, C. T.; Aiken, G. R.; Chalmers, A. T.; Towse, J. E.;
595 Selvendiran, P. Mercury dynamics in relation to dissolved organic carbon concentration and
596 quality during high flow events in three northeastern US streams. *Water Resource. Res.* **2010**,
597 *46*, 1-15.
598 46. Driscoll, C. T.; Yan, C.; Schofield, C. L.; Munson, R.; Holsapple, J. The mercury cycle and fish in
599 Adirondack lakes. *Environ. Sci. Technol.* **1994,** *28*, 136-143.
600 47. King, J. K., Kostka, J. E.; Frischer, M. E.; Saunders, F. M. Sulfate-reducing bacteria methylate
601 mercury at variable rates in pure culture and in marine sediments. *Appl. Environ. Microbiol.*
602 **2000**, *66*, 2430-2437.
603 48. King, J. K.; Kostka, J. E.; Frischer, M. E.; Saunders, F. M.; Jahnke, R. A. A quantitative relationship
604 that demonstrates mercury methylation rates in marine sediments are based on the
605 community composition and activity of sulfate-reducing bacteria. *Environ. Sci. Technol.* **2001**,
606 *35*, 2491-2496.
607 49. Landis, M. S.; Pancras, J. P.; Graney, J. R.; Stevens, R. K.; Percy, K. E.; Krupa, S. Receptor
608 modeling of epiphytic lichens to elucidate the sources and spatial distribution of inorganic air
609 pollution in the Athabasca oil sands region. In *Alberta oil sands: Energy, industry and the*
610 *environment*; Percy, K. E., Eds.; Elsevier: Kidlington, Oxford 2012**;** pp 427-467.
611 50. Constant, P.; Poissant, L.; Villemur, R.; Yumvihoze, E.; Lean, D. Fate of inorganic mercury and
612 methyl mercury within the snow cover in the low arctic tundra on the shore of Hudson Bay
613 (Québec, Canada). *J. Geophys. Res. Atmos. (1984–2012).* **2007**, *112*, D08309.
614 51. Larose, C.; Dommergue, A.; De Angelis, M.; Cossa, D.; Averty, B.; Marusczak, N.; Soumis, N.;
615 Schneider, D.; Ferrari, C. Springtime changes in snow chemistry lead to new insights into
616 mercury methylation in the Arctic. *Geochim. Cosmochim. Acta*. 2010, 74, 6263-6275.
617 52. Barkay, T.; Niels, K.; Poulain, A. J. Some like it cold: microbial transformations of mercury in
618 Polar Regions. *Polar Res*. **2011**, *30*, 15469.

53. Dommergue, A.; Larose, C.; Faïn, X.; Clarisse, O.; Foucher, D.; Hintelmann, H.; Schneider, D.; Ferrari, C. P. Deposition of mercury species in the Ny-Ålesund area (79 N) and their transfer during snowmelt. *Environ. Sci. Technol*. **2009**, *44*, 901-907.
54. Hammerschmidt, C. R.; Lamborg, C. G.; Fitzgerald, W. F. Aqueous phase methylation as a potential source of methylmercury in wet deposition. Atmos. Environ. 2007, 41, 1663-1668.
55. Hintelmann, H. Organomercurials: their formation and pathways in the environment. *Met. Ions. Life. Sci.* **2010**, *7*, 365-401.
56. Kelly, C. A.; Rudd, J. W. M.; St. Louis, V. L.; Heyes, A. Is total mercury concentration a good predictor of methyl mercury concentration in aquatic systems? In *Mercury as a Global Pollutant;* Porcella, D.B., Huckabee, J.W., Wheatley, B., Eds.; Springer Netherlands 1995; pp. 715-724.
57. Rudd, J. W. M. Sources of methyl mercury to freshwater ecosystems: A review. *Water Air Soil Pollut.* **1995**, *80*, 697-713.
58. Eckley, C. S.; Hintelmann, H. Determination of mercury methylation potentials in the water column of lakes across Canada. *Sci. Tot. Environ*. **2006**, *368*, 111-125.
59. Canadian Council of Ministers of the Environment (CCME); http://st-ts.ccme.ca/.
60. Alexander, A. C.; Chambers, P. A. Water quality patterns in 7 rivers in the Canadian oil sands region 1972 to 2010. *In preparation*.

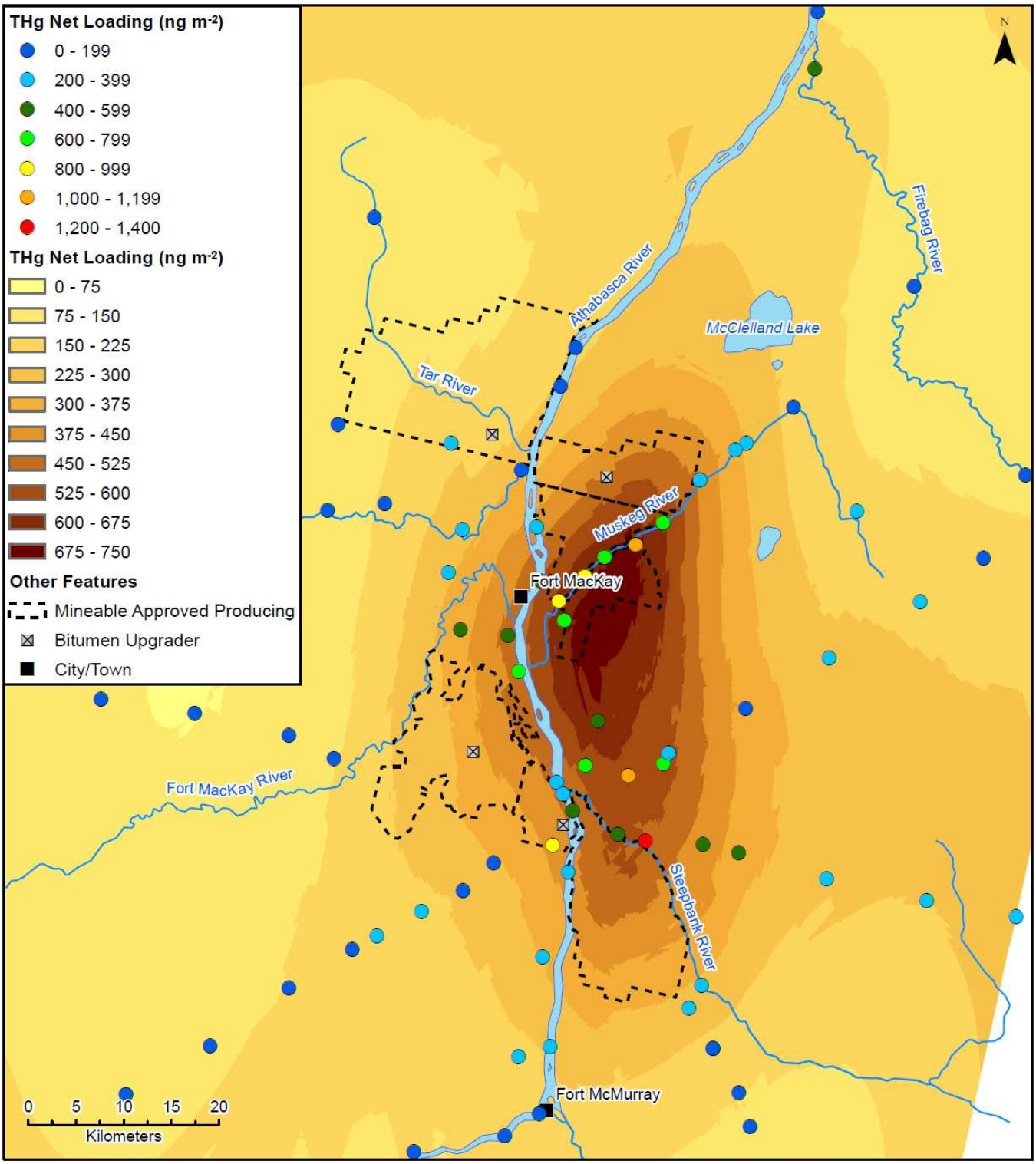
THg Net Loading (ng m-2)
0 - 199
200 - 399
400 - 599
600 - 799
800 - 999
1,000 - 1,199
1,200 - 1,400
THg Net Loading (ng m-2)
0 - 75
75 - 150
150 - 225
225 - 300
300 - 375
375 - 450
450 - 525
525 - 600
600 - 675
675 - 750
Other Features
Mineable Approved Producing
Bitumen Upgrader
City/Town
N
Athabasca River
Firebag River
McClelland Lake
Tar River
Muskeg River
Fort MacKay
Fort MacKay River
Steepbank River
Fort McMurray
0 5 10 15 20
Kilometers

640

641

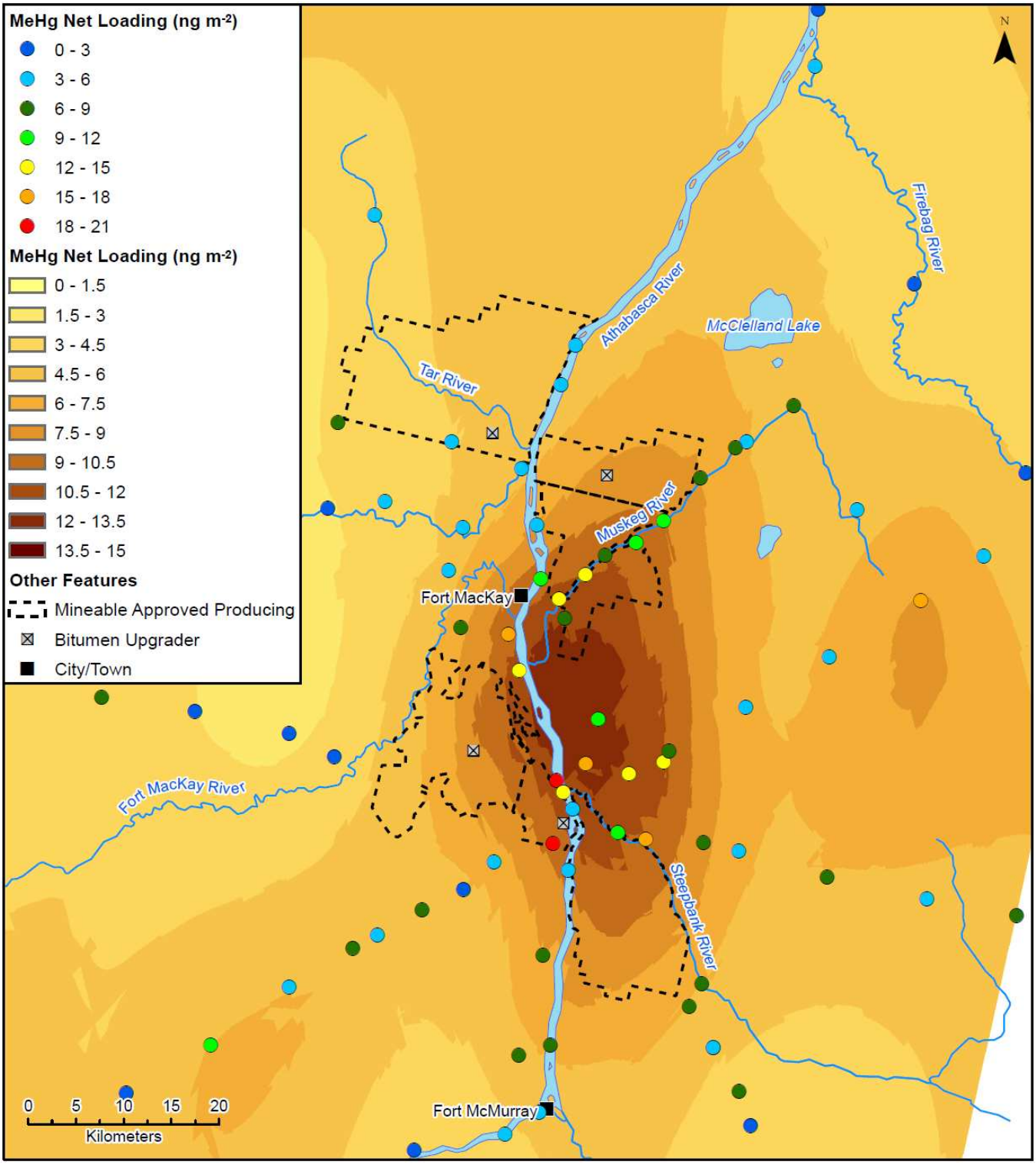

642

643 Figure 1. Kirk et al.

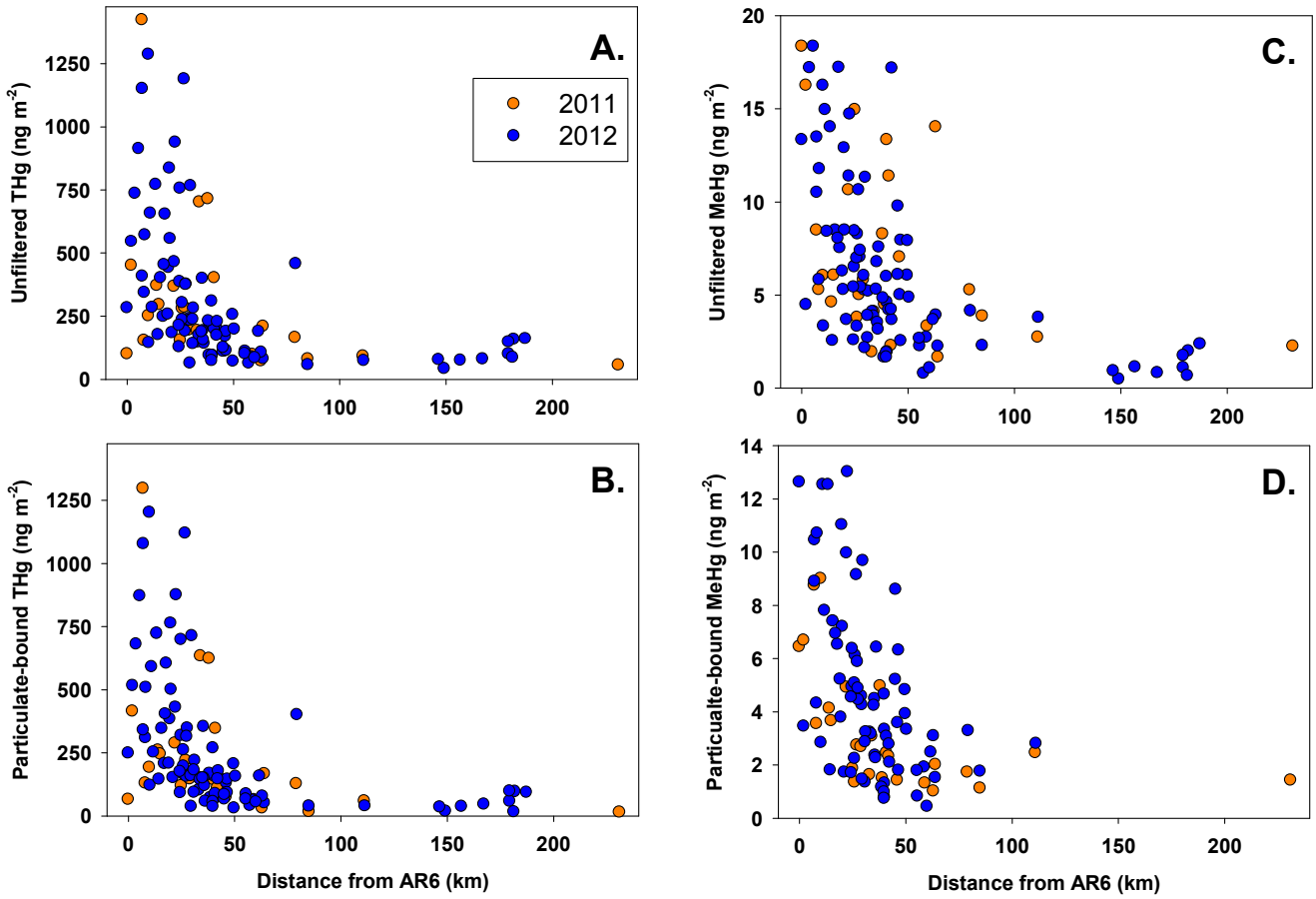

Figure 2. Kirk et al.

656 Table of Contents art:

657

658

659

660

661